جامعة الملك عبدالله
للعلوم والتقنية
King Abdullah University of
Science and Technology

Large Area Deposition of MoS2 by Pulsed Laser Deposition with In-Situ Thickness Control

Item Type	Article
Authors	Serna, Martha I.; Yoo, Seong H.; Moreno, Salvador; Xi, Yang; Oviedo, Juan Pablo; Choi, Hyunjoo; Alshareef, Husam N.; Kim, Moon J.; Minary-Jolandan, Majid; Quevedo-Lopez, Manuel A.
Citation	Large Area Deposition of MoS2 by Pulsed Laser Deposition with In-Situ Thickness Control 2016 ACS Nano
Eprint version	Post-print
DOI	10.1021/acsnano.6b01636
Publisher	American Chemical Society (ACS)
Journal	ACS Nano
Rights	This document is the Accepted Manuscript version of a Published Work that appeared in final form in Large Area Deposition of MoS2 by Pulsed Laser Deposition with In-Situ Thickness Control, copyright © American Chemical Society after peer review and technical editing by the publisher. To access the final edited and published work see http://pubs.acs.org/doi/abs/10.1021/acsnano.6b01636.
Download date	09/08/2022 19:22:26
Link to Item	http://hdl.handle.net/10754/611336

ACS NANO

Subscriber access provided by King Abdullah University of Science and Technology Library

Article

Large Area Deposition of MoS by Pulsed Laser Deposition with In-Situ Thickness Control

Martha I. Serna, Seong H. Yoo, Salvador Moreno, Yang Xi, Juan Pablo Oviedo, Hyunjoo Choi, Husam N. Alshareef, Moon J. Kim, Majid Minary-Jolandan, and Manuel A. Quevedo-Lopez

ACS Nano, **Just Accepted Manuscript** • DOI: 10.1021/acsnano.6b01636 • Publication Date (Web): 24 May 2016

Downloaded from http://pubs.acs.org on May 31, 2016

Just Accepted

"Just Accepted" manuscripts have been peer-reviewed and accepted for publication. They are posted online prior to technical editing, formatting for publication and author proofing. The American Chemical Society provides "Just Accepted" as a free service to the research community to expedite the dissemination of scientific material as soon as possible after acceptance. "Just Accepted" manuscripts appear in full in PDF format accompanied by an HTML abstract. "Just Accepted" manuscripts have been fully peer reviewed, but should not be considered the official version of record. They are accessible to all readers and citable by the Digital Object Identifier (DOI®). "Just Accepted" is an optional service offered to authors. Therefore, the "Just Accepted" Web site may not include all articles that will be published in the journal. After a manuscript is technically edited and formatted, it will be removed from the "Just Accepted" Web site and published as an ASAP article. Note that technical editing may introduce minor changes to the manuscript text and/or graphics which could affect content, and all legal disclaimers and ethical guidelines that apply to the journal pertain. ACS cannot be held responsible for errors or consequences arising from the use of information contained in these "Just Accepted" manuscripts.

ACS Publications

ACS Nano is published by the American Chemical Society. 1155 Sixteenth Street N.W., Washington, DC 20036

Published by American Chemical Society. Copyright © American Chemical Society. However, no copyright claim is made to original U.S. Government works, or works produced by employees of any Commonwealth realm Crown government in the course of their duties.

1
2
3
4
5
6
7
8
9
10
11
12
13
14
15
16
17
18
19
20
21
22
23
24
25
26
27
28
29
30
31
32
33
34
35
36
37
38
39
40
41
42
43
44
45
46
47
48
49
50
51
52
53
54
55
56
57
58
59
60

Large Area Deposition of MoS_2 by Pulsed Laser Deposition with *In-Situ* Thickness Control

Martha I. Serna[†], *Seong H. Yoo*[‡], *Salvador Moreno*[††‖], *Yang Xi*[†], *Juan Pablo Oviedo*[†], *Hyunjoo Choi*[‡], *Husam N. Alshareef*[~], *Moon J. Kim*[†], *Majid Minary-Jolandan*[††,‖], *Manuel A. Quevedo-Lopez*[†]*

[†]Materials Science and Engineering Department, The University of Texas at Dallas, Richardson TX 75080. USA

[‡]Department of Advanced Materials Engineering, Kookmin University, Jeongneung-dong Seongbuk-gu, Seoul 136-702, South Korea

[‖]Department of Mechanical Engineering, The University of Texas at Dallas, Richardson, TX 75080. USA

[~]King Abdullah University of Science and Technology (KAUST), Thuwal, Saudi Arabia.

Alan G. MacDiarmid NanoTech Institute, The University of Texas at Dallas, Richardson, TX 75080. USA

*Corresponding author: mquevedo@utdallas.edu

Keywords: 2D Materials, MoS_2, Pulsed Laser Deposition (PLD), Engineered Target, Electrical Properties, Layered Materials.

ABSTRACT: A scalable and catalyst-free method to deposit stoichiometric Molybdenum Disulfide (MoS_2) films over large areas is reported with the maximum area limited by the size of the substrate holder. The method allows deposition of MoS_2 layers on a wide range of substrates without any additional surface preparation including single crystals (sapphire and quartz), polycrystalline (HfO_2), and amorphous (SiO_2). The films are deposited using carefully designed MoS_2 targets fabricated with excess of sulfur (S) and variable MoS_2 and S particle size. Uniform and layered MoS_2 films as thin as two monolayers, with an electrical resistivity of 1.54×10^4 Ω cm^{-1} were achieved. The MoS_2 stoichiometry was as confirmed by High Resolution Rutherford Backscattering Spectrometry (HRRBS). With the method reported here, *in situ* graded MoS_2 films ranging from ~1 to 10 monolayers can also be deposited.

Recent advancements in 2D materials have created great opportunities for devices based on single semiconductor, dielectric and conductive layers.[1] Some of these opportunities include the development of new generation of sensors, transistors and high performance devices with superior performance compared to those fabricated with bulk materials due to the high quantum efficiency in 2D materials. [2,3,4] Some of the most common 2D materials include graphene, molybdenum disulfide (MoS_2), Tungsten disulfide (WS_2), among others. Unlike graphene, the band gap of transition metal di-chalcogenides (TMDs) can be tuned from direct to indirect by simply varying the number of layers.[5] Among 2D-TMD materials, layered MoS_2 films are the most extensively studied.[6-9] Some of the MoS_2 applications reported include gas sensors,[10] phototransistors,[2] flexible thin film transistors,[11] electrodes for lithium ion batteries,[12] and heterojunctions diodes with black phosphorous.[13]Recently, the piezoelectric effect in monolayer MoS_2 was also reported.[14]2D MoS_2 films incorporated as the active layer in thin film transistors have shown mobilities of ~200 cm^2 / V-s and on/off current ratio of $\sim 1\times10^8$ with HfO_2 as the gate insulator.[15] More recently, mobilities of ~480 cm^2 / V s (holes) and ~470 cm^2 / V s (electrons) for MoS_2 on PMMA substrates was reported.[16] These materials are also theoretically ideal for Field Effect transistors (FET) with dimensions of less than 10 nm since the use of these materials greatly reduce short channel effects without affecting the Drain-Induced Barrier Lowering (DIBL, ~10 mV / V). [17] Besides the exciting applications mentioned above new applications for 2D MoS_2 are continuously reported. However, any practical applications of 2D-

1
2
3
4
5
6
7
8
9
10
11
12
13
14
15
16
17
18
19
20
21
22
23
24
25
26
27
28
29
30
31
32
33
34
35
36
37
38
39
40
41
42
43
44
45
46
47
48
49
50
51
52
53
54
55
56
57
58
59
60

MoS_2 require the growth of high quality and large area compatible films to enable reliable and reproducible devices at a reasonable cost.

Some of the fabrication methods reported for 2D MoS_2 include mechanical exfoliation,[18] laser thinning,[19] chemical vapor deposition (CVD),[20-22] chemical bath deposition,[23] liquid exfoliation,[24, 25] and Lithium intercalation.[26] Mechanical exfoliation produces monolayers and multilayers with excellent quality; however, this method lacks precise control of the exfoliated area, geometry, size, and consistency among number of layers. Laser thinning, although relatively new, often results in increased roughness of up to three orders of magnitudes of the MoS_2 films after thinning.[27]

In this article, we report PLD methods for the fabrication of MoS_2 films. Using PLD for layered MoS_2 films offers several advantages. For example, during laser deposition the ablated species from the target are often activated. This results in enhanced associative chemistry on the growing film surface that reduces the need for surface activation.[28] Also, thickness control is achieved by controlling the growth kinetics by simply manipulating the repetition rate (frequency) and energy of the laser as well as the deposition pressure. One additional advantage of PLD is the stoichiometric transfer of the ablated material from the target to the substrate. This characteristic is a consequence of ablation produced by the absorption of the laser energy on a very small volume of the target. The absorption of the laser energy by this small volume consequently forms a plasma, or plume, at the surface of the target and the species get transferred to the substrate. This process is not dependent on the partial pressures of the constituent cations.[29] However, the deposition pressure can be used to modify the mean free path of the ablated species to either minimize or maximize the energy of the species reaching the surface of the substrate. In PLD processes, only the stoichiometry is transferred from the target to the substrate and the crystalline phase of the resulting film is not necessarily the same as that of the target.[29] Avoiding expensive and potentially dangerous precursors (See the Supplementary Information for approximate costs) is additional advantage of this technique over other methods such as CVD.

Earlier reports of MoS_2 deposited by PLD focused on films deposited on stainless steel for tribological applications and the process resulted in films with increased sulfur vacancies as the

substrate temperature increased.[30,31] Although this might not be an issue for tribological applications, Sulfur deficiency or Oxygen contamination can have a negative effect on the electrical properties of 2D MoS_2 films. MoS_3 conversion to MoS_2 using laser annealing has also been reported.[32] The annealing process generated heterogeneous MoS_2 films with amorphous Sulfur incorporated in the bulk of the MoS_2, producing inadequate films for device applications. However, through fine-tuning of the PLD deposition parameters and proper target preparation, such defects may be avoided. The selection of the deposition parameters must allow the Mo and S species to properly arrange on the substrate during the deposition and substrate cooling process. Special considerations for MoS_2 deposition by PLD on metallic substrates must be considered. For example, MoS_2 deposited on Ni and Ag substrates form NiS_2 and AgS_2.[33] Multilayered MoS_2 by PLD was also demonstrated on Al_2O_3, GaN, and SiC-6h substrates.[34-37]

In those studies, although layered MoS_2 films were obtained, the HRBS stoichiometric analysis of the resulting MoS_2 films were not reported.

RESULTS AND DISCUSSION

In this work, a large-area compatible process to deposit stoichiometric MoS_2 with layers ranging from 1-10 is reported. This is achieved by properly controlling target composition, MoS_2 to Sulfur particle size in the target, and PLD deposition conditions. 1.33 nm thick MoS_2 films and Mo/S ratio of ~0.5 can be achieved with the method reported here. Furthermore, this process can be used to deposit layered MoS_2 on amorphous, polycrystalline and single crystal substrates. PLD deposition conditions evaluated to enable layered MoS_2 include cooling rate of the substrate, laser fluency and deposition pressure. These parameters were optimized to allow the nucleation and arrangement of the MoS_2 layers on the substrate. Three different targets with excess of Sulfur were used to compensate the potential loss of this element during the laser ablation. The combination of target composition and proper PLD conditions results in deposition of MoS_2 films on ~50.8 mm diameter substrates. In addition, the influence of the target characteristics on the chemistry, crystallinity, and electronic properties of the layered MoS_2 films was studied. An additional advantage of the method reported here is the capability of tuning the MoS_2 thickness across the entire substrate by simply modifying the PLD deposition conditions.

1
2
3
4
5
6
7
8
9
10
11
12
13
14
15
16
17
18
19
20
21
22
23
24
25
26
27
28
29
30
31
32
33
34
35
36
37
38
39
40
41
42
43
44
45
46
47
48
49
50
51
52
53
54
55
56
57
58
59
60

This enables *in situ* thickness gradient control on a whole substrate and under the same deposition conditions.

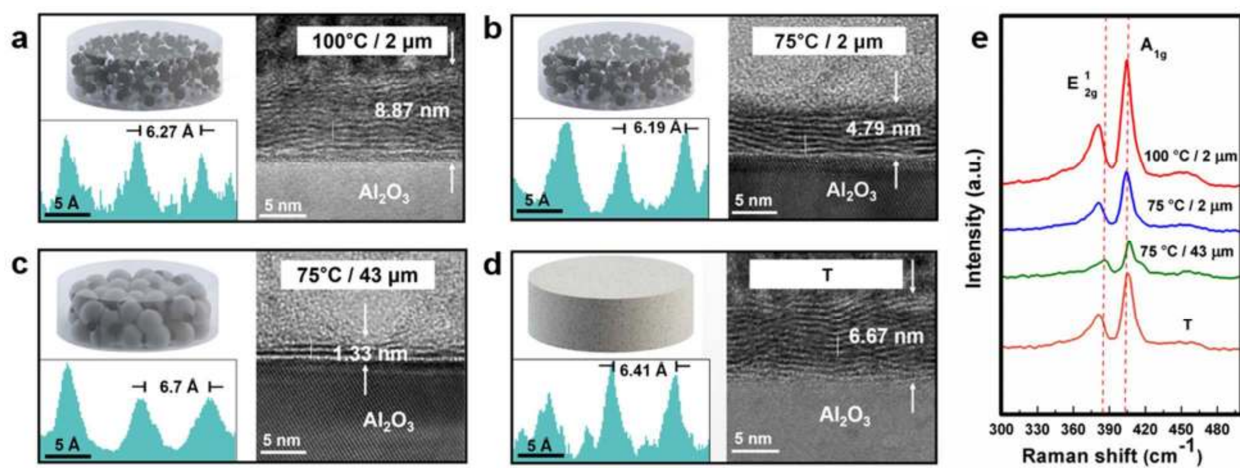

Figure 1. MoS_2: S targets, Transmission Electron Microscopy (TEM) for the MoS_2 films deposited from the different targets, and Raman spectra of the thin films. (a) to (d) show PLD targets, TEM cross-sections and interlayer spacing for films deposited using targets fabricated at 100°C / 2 µm, 75°C / 2 µm, 75°C / 43 µm, and the commercially available target. The thinnest MoS_2 film (c) was deposited from the target with the highest density and larger MoS_2 particles (43 µm). Raman spectra (e) acquired for the MoS_2 shown in Figures a-d. For reference, the dashed lines in Figure 1e show the Raman shift values for a monolayer of MoS_2.

Targets fabrication for the stoichoimetric MoS_2 synthesis by PLD

Conventional powder metallurgy methods were used to fabricate the PLD targets with MoS_2 to S ratio of 1:1. Particle size for the target preparation was 20 µm (Sulfur) and 43 and 2 µm (MoS_2). Two different hot press conditions for the target fabrication were evaluated: a) 100°C and compression of 25 tons per one hour, and b) 75°C with compression of 18 tons for 3 hours **(Figure S1).** For comparison, a commercial MoS_2 target with no excess of Sulfur (MoS_2 to S ratio of 1:0) from Testbourne Ltd was used. This is referred as target "T" in this article. The 3 targets fabricated for this work are identified as follows: 100ºC / 2 µm, 75ºC / 2 µm, and 75ºC / 43 µm. A detailed outline of the target preparation conditions is shown in Table 1 in the Supporting Information section. The relative density of each target was measured by Archimedes

principle and defined as the ratio of the experimental and theoretical density values. Relative densities of 88.1%, 88.7% and 99.9% were obtained for targets 100°C / 2 µm, 75°C / 2µm, and 75°C / 43µm, respectively. It is important to note that the 100°C / 2 µm and 75°C / 2 µm have the same S particle size (**Figure S2)**. The difference in the density with respect to the 75°C / 43µm target is due to the MoS_2 particle size and target fabrication conditions.

Thin film Thicknesses and cross section - layered structure

All the targets described before were used to initially deposit MoS_2 films by PLD on sapphire (single crystal). The cross-section for each MoS_2 film was obtained using Transmission Electron Microscopy (TEM) (**Figure 1a to 1d)**. MoS_2 films with thicknesses of 8.87 nm, 4.79 nm, 1.33 nm and 6.67 nm were obtained for films deposited from targets 100°C / 2 µm, 75°C / 2 µm, 75°C / 43µm and T, respectively. The TEM results showed that MoS_2 films obtained from targets 100°C/ 2 µm, 75°C / 2 µm, and T have a well-defined layered structure with some areas showing a wavy-like structure. Nevertheless, layered films were observed for all these films. Films obtained from the target with the largest MoS_2 particle size (75°C / 43 µm) showed the thinnest and most ordered layered structure (**Figure 1d)**. The interlayer spacing evaluated from the TEM images were 6.27, 6.19, 6.70, and 6.41 Å for 100°C / 2 µm, 75°C / 2 µm, 75°C / 43 µm, and T, respectively. These values are very close to the theoretically expected value for monolayers of MoS_2 which is ~6.5 Å.[8] The small variations observed are likely due to the resolution of the TEM measurement and/or to small local stoichiometry variation in the films due to Sulfur depleted areas, which will be further discussed in the following sections.

Thin films chemical characterization

The Raman spectroscopy analyses of the films showed the typical E^1_{2g} and A_{1g} vibration modes for MoS_2 **(Figure 1e)**. The red dashed lines in the **Figure 1e** indicate the expected vibration modes values for a monolayer of MoS_2.[38] The additional vibration bands observed for this films are from the sapphire (Al_2O_3) substrate.[37] The difference in frequency in the MoS_2 vibration modes, defined as $\Delta\beta$, is proportional to the separation of the Raman peaks and can be used to estimate the thickness of the films.[38] The difference in the $\Delta\beta$ values with thickness is due to the dipolar interaction of the substrate with the MoS_2 thin film due to variations in the electrostatic surroundings and interaction between the substrate and the Sulfur atoms. This affects the MoS_2

1
2
3
4
5
6
7
8
9
10
11
12
13
14
15
16
17
18
19
20
21
22
23
24
25
26
27
28
29
30
31
32
33
34
35
36
37
38
39
40
41
42
43
44
45
46
47
48
49
50
51
52
53
54
55
56
57
58
59
60

vibration modes.[40] The Δβ values calculated from **Figure 1e** were 24 cm^{-1}, 23 cm^{-1}, 20 cm^{-1}, and 24 cm^{-1} for thin films 100°C / 2 μm, 75°C / 2 μm, 75°C / 43 μm and T, respectively. The expected Δβ values as function of number of layers are: 18 cm^{-1} (one layer), 22.4 cm^{-1} (two layers), 23 cm^{-1} (3 monolayers), and 25 cm^{-1} for bulk MoS_2.[38] From the TEM data, it is clear that films 100ºC / 2 μm, 75 ºC / 2 μm , and T are relatively thick and, therefore, show Δβ values closer to bulk MoS_2. However, thin film 75°C / 43 μm showed the lowest value for Δβ (~20 cm^{-1}) indicating that this is the thinnest film and in the order of 1-2 monolayers. This is in agreement with the TEM results shown in **Figure 1c**.

In general, the thickness of the MoS_2 films are inversely proportional to the density of the target Therefore, the target with the highest density (75°C / 43 μm) yielded the thinnest MoS_2 films. The thinner MoS_2 films resulting from targets with higher density is likely due to lower ablation rates from denser targets. Additionally, besides producing thicker MoS_2 films, low-density targets also produced more particles on the MoS_2 surface **(Figure S2).**[41] Excess of Sulfur was used to saturate the deposition ambient and minimize vacancies in the MoS_2 films. During the ablation, the excess of Sulfur from the target evaporates more readily than the MoS_2 producing and *in-situ* sulfurization environment allowing more stoichiometric MoS_2 to be deposited on the substrate. We used an RGA system (Residual Gas Analyzer) during the deposition to monitor the increase in Sulfur partial pressure during the ablation.

1
2
3
4
5
6
7
8
9
10
11
12
13
14
15
16
17
18
19
20
21
22
23
24
25
26
27
28
29
30
31
32
33
34
35
36
37
38
39
40
41
42
43
44
45
46
47
48
49
50
51
52
53
54
55
56
57
58
59
60

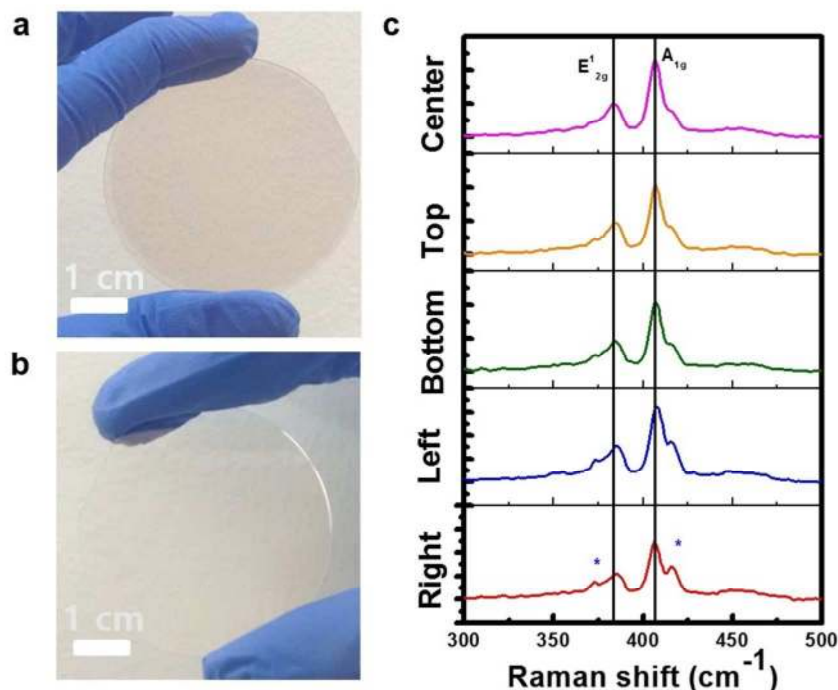

Figure 2. (a) 1.33 nm thick (2 monolayers) MoS_2 thin film deposited by PLD on a 50.8 mm diameter sapphire wafer. (b) Sapphire wafer without MoS_2 thin film (c) Raman spectroscopy from the MoS_2 films. (a) Shows that the characteristic E^1_{2g} and A_{1g} vibration modes for MoS_2 are present across the entire surface of the substrate. The (*) shows the vibration modes for sapphire

Large area depositions were performed on 50.8 mm sapphire substrates using the target with the highest density (75°C / 43 µm). This target was selected because it yielded the thinnest MoS_2 film **(Figure 2a)**. For large area PLD deposition of thin films on large substrates, a laser deposition power of less than 6W is recommended.[42] Therefore, the power used in the deposition reported in this paper was set to 3W. This PLD deposition power yields MoS_2 films, as shown in the optical image shown in **Figure 1a**, the whole sapphire wafer **(Figure 2b)** was covered with exception on the small wafer edges that were suspended on the substrate holder during the deposition **(Figure S3)**. The Raman spectroscopy obtained in different areas of the same substrate: top, bottom, left side, right side and center of the wafer **(Figure 2b)**. All areas showed the E^1_{2g} and A_{1g} MoS_2 vibration modes indicating presence of the MoS_2 thin film on the wafer area. The overall thickness of the films, as measured by TEM was 1.33 nm, or close to 2 monolayers. The (*) represents the vibration modes E_{1g} (~379 cm^{-1}) and A_{1g} (~416 cm^{-1}) for the

sapphire substrate.[43] The variation of the intensity of these peaks can be evidence of little defects or our thin films.

X-ray photoelectron spectroscopy (XPS) studies were further used to analyze the films after a subtle sputter-clean with Ar^+ ions. The Mo 3d region shown in **Figure S4a** showed typical binding for MoS_2 (red dashed lines) for thin films deposited from targets 100 ºC / 2 μm and T. The small variation in the S2p region observed in **Figure S4b** for films deposited from targets 75 ºC / 2 μm and T can be attributed to Fermi level pinning due to sulfur vacancies.[44] Nevertheless, all the thin films showed bands typical for MoS_2 **(Figure S5)**. The data fitting shows some low intensity oxides peaks (MoO_2 and MoO_3) for all the films, with the highest concentration for the films deposited from the commercial target, T. Thin film 75 ºC / 43 μm was not subjected to sputter cleaning due to its thickness, but showed the closest binding energies to bulk MoS_2.

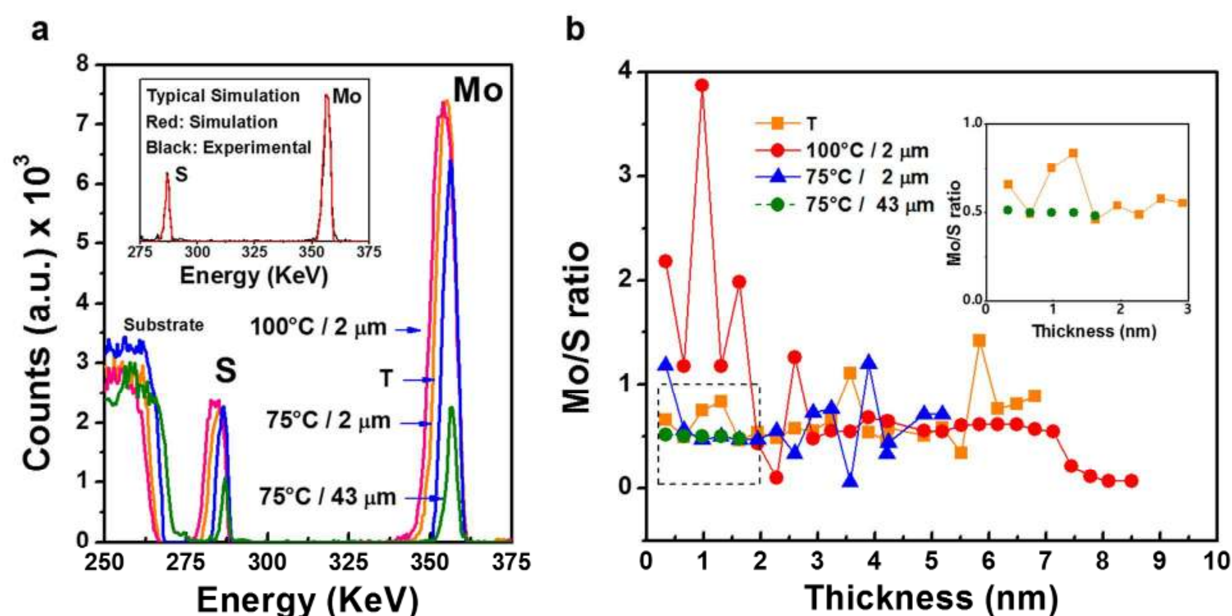

Figure 3. Rutherford Backscattering Spectra for the MoS_2 films. (a) Experimental spectra. The inset shows the experimental spectra (continuous dark line) and simulation spectra (red line) for thin film 75 ºC / 43 μm. (See Figure S6 for simulations details for all the films). The Mo/S ratio depth profiling for all the MoS_2 thin films on sapphire was measured (b). The inset shows the zoomed-in view for 75°C / 43 μm (green) and the commercial target (T).

High-Resolution Rutherford Backscattering (HRRBS) analyses were performed to better evaluate the composition of the MoS_2 films **(Figure 3a)**. Peaks for S, Mo and the substrate are clearly observed in the experimental data. The difference in peak width and intensity observed in the HRRBS spectra is related to the thickness of the MoS_2. The thinnest film was obtained from 75 ºC / 43 μm target, in agreement with Raman and TEM. The HRRBS experimental data was fitted to obtain the depth profile for each film. The inset in **Figure 3a** shows typical fits (red line) and experimental data (black line). The depth profile extracted from the fitting is shown in **Figure 3b**. Thin film 100 ºC / 2 μm shows a large depletion of S at the surface with composition variation throughout the entire thickness of the thin film. Thin film 75 ºC / 2 μm showed higher Mo/S ratios close to the surface, but from 1.0 to 2.2 nm the Mo/S ratio approached the theoretical ratio of 0.5. The film from the commercial target (T) also showed variations in the Mo/S ratio**.** On the other hand, thin film 75 ºC / 43 μm showed ratios close to 0.5 throughout the entire thickness of about 2 monolayers. The inset in **Figure 3b** shows the stoichiometricity of these films over the entire thickness. The complete HRRBS spectra and simulations are shown in **Supporting Information Figure S6.**

1
2
3
4
5
6
7
8
9
10
11
12
13
14
15
16
17
18
19
20
21
22
23
24
25
26
27
28
29
30
31
32
33
34
35
36
37
38
39
40
41
42
43
44
45
46
47
48
49
50
51
52
53
54
55
56
57
58
59
60

Thin film resistivity and Mo / S ratio

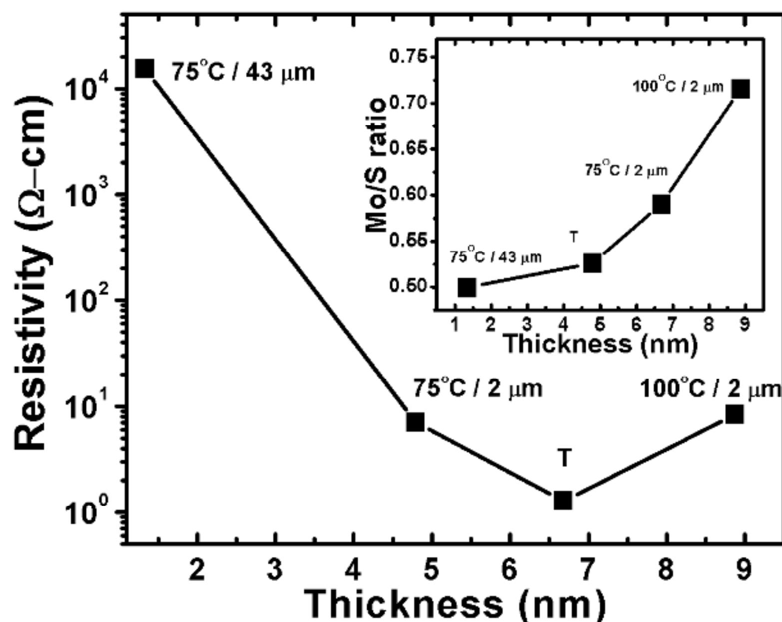

Figure 4. Resistivity and Mo/S atomic ratio for thin films 100ºC / 2µm, 75ºC / 2µm, 75ºC / 43 µm and T is shown. The Mo/S ratio is closer to the ideal value of 1:2 (0.5) for thinner films and the contact resistivity increases as the thickness is reduced. This shows a relationship between the content of Sulfur and the contact resistivity of the films. The 75ºC / 43 µm film, which is the thinnest, has an approximate ratio of 0.5 and highest resistivity (~10^4 Ω-cm).

The mechanisms for electronic transport in 2D materials are not entirely clear yet since the carrier transport in layered MoS_2 films as well as in the contact interface is very complex. [8, 45-48] In this paper, we used a well-accepted method (Circular Transfer Method, CTLM) to measure sheet resistance and resistivity that eliminates potential contact resistance issues while performing the measurement. Gold contacts were used for the analyses **(Figure S7)**. The results were then correlated to the Mo/S ratio in each film**.** For the CTLM method, the I -V responses of the structured were measured at room temperature and in air**.** From these data, electrical resistivity values of 8.0, 7.0, 1.3, and 1.54×10^4 Ω cm^{-1} were obtained for 100 ºC / 2 µm, 75 ºC / 2 µm, T, and 75 ºC / 43 µm films, respectively **(Figure 4)**.

1
2
3
4
5
6
7
8
9
10
11
12
13
14
15
16
17
18
19
20
21
22
23
24
25
26
27
28
29
30
31
32
33
34
35
36
37
38
39
40
41
42
43
44
45
46
47
48
49
50
51
52
53
54
55
56
57
58
59
60

Clearly, as Mo/S ratio increases the electrical resistivity of the films is reduced. This can be produced by presence of defects on the thin film metal interface too. The area analyzed by both Raman (~ 2 x 10^9 μm^2) and HRRBS (9 x 10^6 μm^2) is much larger that the size of the CTLM structure used for the measurements, which is 1.2 x 10^6 μm^2 **(Figure S8)** which is considerable larger that commonly exfoliated MoS_2 flakes.[49] In addition, The sheet resistance (R_{sh}) values reported in this paper are 1.15 X 10^{11} Ω /sq., 1.4 X 10^7Ω / sq., 9.4 X 10^4Ω / sq., and 1.9 X 10^6 Ω / sq., for films 75ºC / 43µm, 75ºC / 2µm, 100ºC / 2µm, and T, respectively. These large values for sheet resistance might indicate uniform MoS_2 films on the analyzed areas. For reference, the largest sheet resistance for large area deposition of MoS_2 by Chemical Vapor Deposition reported range from 1.46 - 2.84 x 10^7 Ω/ sq.[50] Furthermore, the values of R_{sh} and ρ are much larger for bilayers than for films with several layers of MoS_2, which has been reported in previous works. [51] The thinnest thin film showed and Mo/S ratio of 0.5, but the material still needs improvement for electronic applications. The changes in resistivity could also affected by defects and impurities at the interface metal – semiconductor as well.[51]

Thin film deposition on different substrates

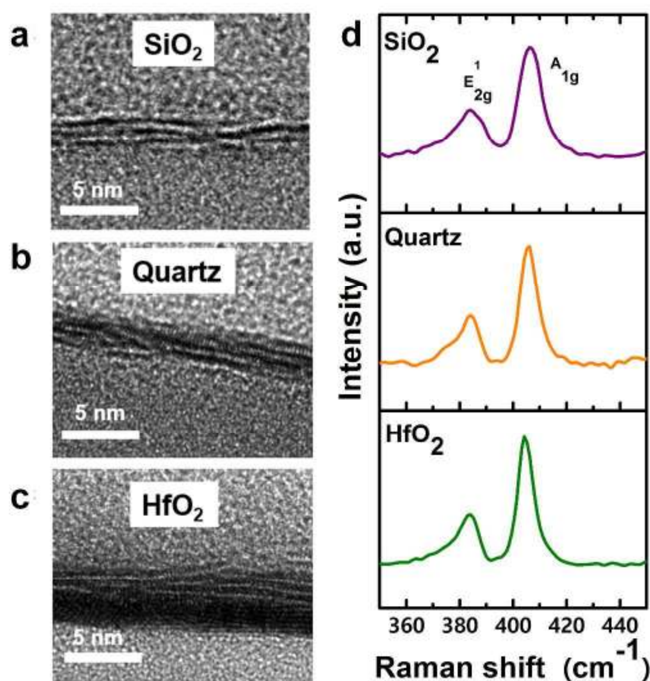

1
2
3
4
5
6
7
8
9
10
11
12
13
14
15
16
17
18
19
20
21
22
23
24
25
26
27
28
29
30
31
32
33
34
35
36
37
38
39
40
41
42
43
44
45
46
47
48
49
50
51
52
53
54
55
56
57
58
59
60

Figure 5. MoS_2 thin films deposited on different substrates. MoS_2 films are achieved on SiO_2 (amorphous) (a), Quartz (single crystal) (b), and HfO_2 (polycrystalline) (c) substrates. The thicknesses of the films were 2.5 nm, 2.8 nm and 2.1 nm for SiO_2, quartz, and HfO_2, respectively.

The PLD method reported here was also used to deposit MoS_2 on various substrates including SiO_2, quartz, and polycrystalline HfO_2 **(Figure 5a-c)**. The films were deposited from the target that produced the most stoichiometric film (75ºC / 43 μm). The quartz substrate had some amorphization during the TEM sample preparation due to the use of Focus Ion Beam (FIB) during sample preparation. The MoS_2 thin films deposited on HfO_2 (**Figure 5c**) seems to have better quality than films deposited on amorphous SiO_2 substrates. These initial outcomes indicate that further improvements in the PLD process for amorphous substrates are required. The thicknesses for the films deposited on SiO_2, quartz, and HfO_2 were 2.5 nm, 2.83 nm, and 2.08 nm, respectively. The films were evaluated by Raman spectroscopy and the vibration modes for MoS_2 were present on all the substrates. However, the Raman bands for MoS_2 on SiO_2 and quartz were broader than those on crystalline HfO_2, indicating better quality of the MoS_2 films deposited on this dielectric **(Figure 5d)**.

In-Situ Thickness Control

The process demonstrated here is also a great method to achieve different MoS_2 thicknesses on the same substrate. Such thickness control can be used to fabricate devices on the same substrate with variable number of MoS_2 layers. The analyses of these films are shown in **Figure 6** with area-1 corresponding to the thickest and area-5 the thinnest MoS_2 films, respectively. Raman spectroscopy (**Figure 6b**) and Raman mapping **(Figure 6c)** was carried on the entire area of the wafer to evaluate the uniformity of the MoS_2 films. The typical modes for MoS_2 (E^1_{2g} and A_{1g}) monotonically decrease with thickness, as expected. In addition, the separation of the peaks ($\Delta\beta$) was also proportional to the thickness of the thin films indicating a thickness gradient across the substrate.[38] For the gradient generation the substrate speed rotation was reduced and it was moved off-axis from the target, followed by a normal process of deposition.

1
2
3
4
5
6
7
8
9
10
11
12
13
14
15
16
17
18
19
20
21
22
23
24
25
26
27
28
29
30
31
32
33
34
35
36
37
38
39
40
41
42
43
44
45
46
47
48
49
50
51
52
53
54
55
56
57
58
59
60

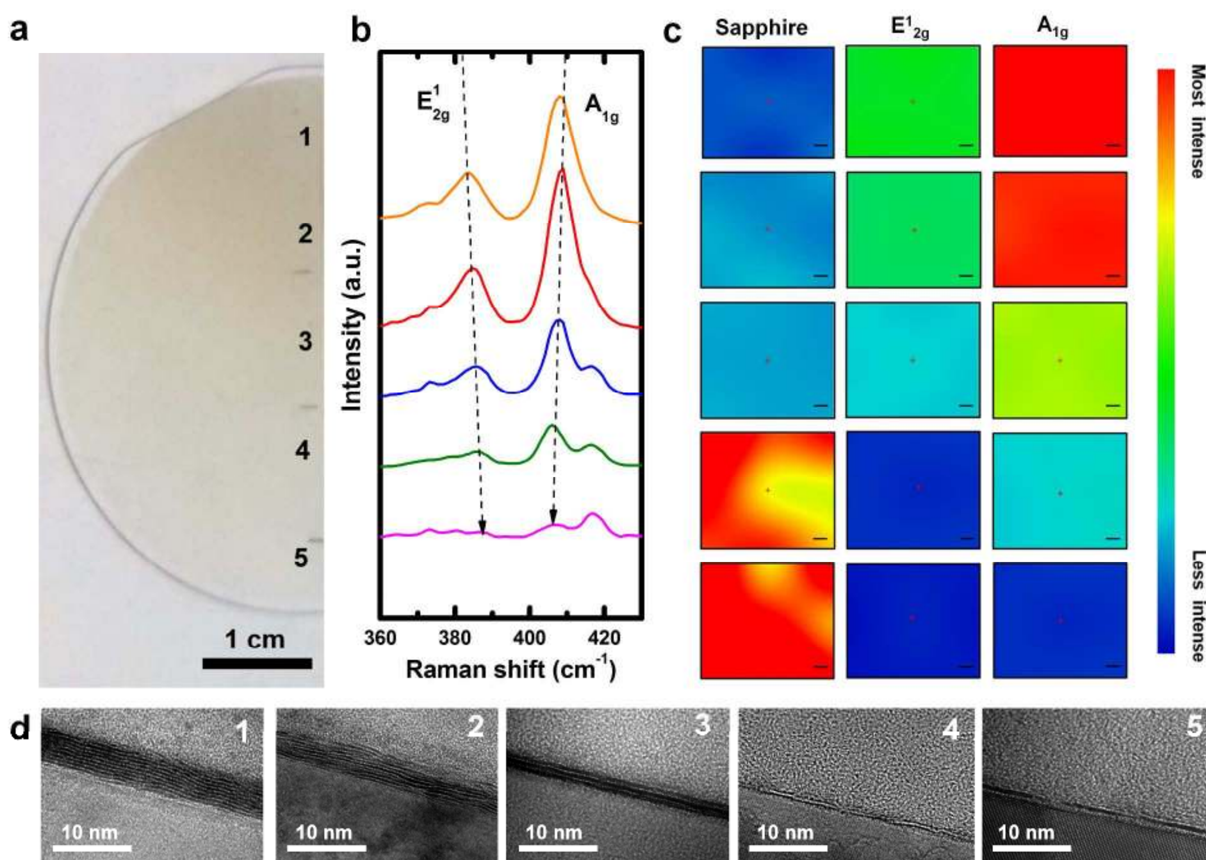

Figure 6. MoS_2 thin film with graded thickness and the corresponding Raman mapping. (a) The optical image shows a MoS_2 thin film thicknesses gradient on half sapphire wafer deposited by PLD thicknesses gradient. Raman spectra and Raman mapping are shown (b-c). Areas of high and low intensity are represented by red and blue colors in the Raman mapping. (d) TEM cross-section results for areas 1 through 5 showing the thickness gradient for the MoS_2 films along the entire substrate. The scale in every Raman mapping picture is 5 µm.

The thickness of each area was approximately: 10 layers, 8 layers, 3, layers, 2 layers and 1 layer for areas 1, 2, 3, 4, and 5, respectively **(Figure 6d)**. These results shows that PLD process is potentially capable of producing a surface on which different electronic structures with several MoS_2 thicknesses can be created and studied.

1
2
3
4
5
6
7
8
9
10
11
12
13
14
15
16
17
18
19
20
21
22
23
24
25
26
27
28
29
30
31
32
33
34
35
36
37
38
39
40
41
42
43
44
45
46
47
48
49
50
51
52
53
54
55
56
57
58
59
60

High Resolution Transmission Electron Microscopy Analyses

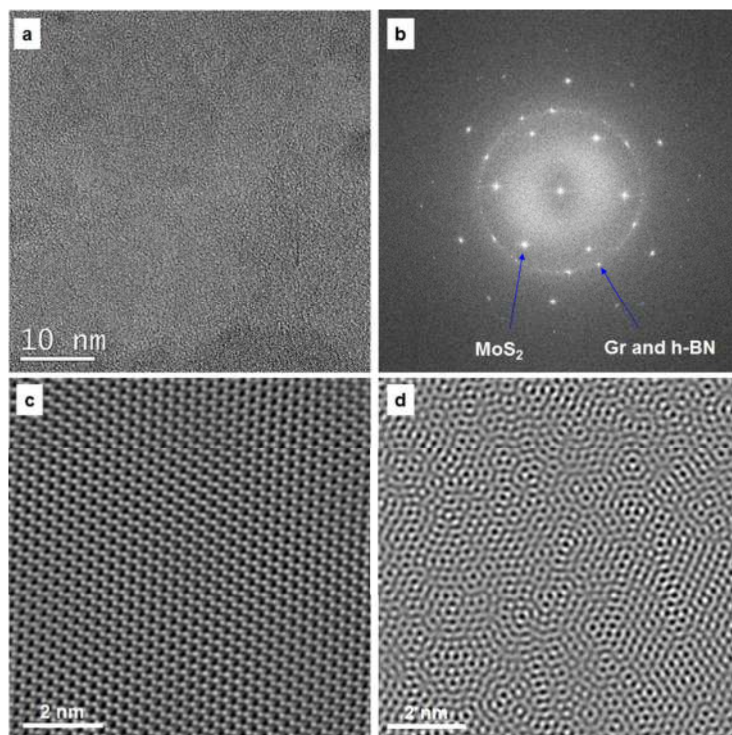

Figure 7. (a) Top view of a 75 ºC / 43 µm MoS2 deposited on h-BN/Graphene. (b) Inversed Fast Fourier Transform (FFT) results. Zoomed FTT images for MoS_2 (c) and MoS_2/h-BN/Gr (d).

In order to evaluate the crystallinity of PLD MoS_2, the thinnest and stoichiometric MoS_2 film (**75 ºC / 43 µm)** sample was deposited on exfoliated Hexagonal Boron Nitride (h-BN) / Graphene (Gr) stack and subjected to TEM analysis. The top view TEM results for the MoS_2 on h-BN/Gr and the corresponding Fast Fourier Transform (FFT) patterns are shown in **Figure 7a-b**, respectively. The inversed FFT patterns in **Figure 7b** reveals the presence of lattices for the MoS_2/h-BN/Gr stack demonstrating the crystalline nature of the films. For reference, the corresponding lattice points for MoS_2 and h-BN/Graphene are shown in **Figure 7b**. Detailed FFT analyses were carried out to separate the signals from MoS_2 and h-BN/Gr (**Figure 7c-d)**. The filtered FFT analyses reveal a crystalline MoS_2 lattice on these substrate **(Figure 7c)**. **Figure 7d** shows the filtered FFT for the entire MoS_2/h-BN/Gr stack. From these results it become clear that it is possible to deposit MoS_2 by PLD in other substrates, especially on other 2D materials such as graphene and h-BN. Furthermore, The Phase contrast imaging of each thin film in this

work deposited on sapphire was checked as well. This imaging showed an atomic arrangement for the thin films **(Figure S9)**.

Furthermore, a 75 ºC / 43 μm film was deposited on Graphene and its top view image showed defined grain boundaries **(Figure S10).** The average grain size was measured resulting in 16.80 nm **(Figure S11 and S12).** The grain size of the stoichiometric thin film synthetized in this work is still smaller than those reported by CVD techniques[52]. However, the continuity of the thin film 75 ºC / 43 μm is found all over the sapphire substrate as demonstrated before.

CONCLUSIONS

A potential process for large-area growth of stoichiometric layered Molybdenum Disulfide (MoS_2) by PLD has been developed. The process uses laser ablation from carefully-designed targets with controlled particle size and Sulfur content. Two One to ten Layers of MoS_2 without any surface preparation can be grown using this process. The high MoS_2 electrical resistivity seems to be related with the stoichiometry of the material, showing that not just density of defects between MoS_2-metal interfaces can have effect on performance of the thin films. Furthermore, MoS_2 growth on amorphous, polycrystalline and single crystal substrates was also demonstrated. With further work, the method reported here can lead to future large-scale deposition of MoS_2 for various applications.

METHODS

Target fabrication: Powder metallurgy was used to fabricate three target types (labeled 100ºC / 2 μm, 75ºC / 2 μm, 75ºC / 43 μm, in this article). Each target has an atomic ratio of MoS_2 to S of 1:1. MoS_2 and S precursors were acquired from Sigma-Aldrich Korea and include MoS_2 with particle size of 43 mm and 2 μm, and S powder with a particle size of 20 μm. To ensure good homogeneity, the MoS_2 and S powders were mixed for one hour before target fabrication on a SPEX mill, SPEX Sample Prep, Inc. model 8000D Dual. The resulting mixed powder was hot-pressed at 75ºC for 3 h at 18 ton-force or 100ºC for 1 h at 25 ton-force. More detailed information regarding this process is discussed in the supporting information.

1
2
3
4
5
6
7
8
9
10
11
12
13
14
15
16
17
18
19
20
21
22
23
24
25
26
27
28
29
30
31
32
33
34
35
36
37
38
39
40
41
42
43
44
45
46
47
48
49
50
51
52
53
54
55
56
57
58
59
60

Thin film deposition: MoS_2 films from each target used in this work were deposited using a KrF laser (λ=248nm) laser. The laser frequency was 10 Hz, with an energy of 30mJ and the substrate temperature was kept at 700°C. The MoS_2 films were deposited on Al_2O_3 (0001) double – side polished substrates (sapphire), HfO_2, Quartz, and SiO_2. Before deposition, the PLD chamber was evacuated to a pressure of $<10^{-6}$ Torr. The process was carried out at 0.1 mTorr without any background gas. After the deposition, the substrate was cooled down at a rate of 2 ºC/min.

Thin film characterization: The first thin films characterization studies were evaluated by Raman spectroscopy Thermo Scientific™ DXR™ Raman microscope with 532 nm excitation and 50X objective. The laser power was kept at 0.3 mW during the experiment. The XPS measurements were executed using a PHI 5000 Versa Probe II. All the evaluations were taken at a 45 take-off angle with respect to the sample surface. A monochromatic Al Kα radiation (hν= 1486.6 eV) was used with a 0.1 eV step size and a pass energy of 23.50 eV. The base pressure in the analysis was $1.6x10^{-8}$ Torr. All binding energies reported in this work are relative to the C 2S peak at a binding energy of 284.8 eV. The cross section of each film was used to examine crystalline structures and thicknesses of the film by high-resolution transmission electron microscope (HRTEM, Tecnai F20 G2, FEI, USA) with an energy dispersive spectroscope (EDS, PV9761/55, Ameteck, USA). The TEM samples were prepared using a focused ion-beam system (FIB) system (Nova nanolab 600, FEI Ltd., USA). The electrical properties of the thin films were studied by Circular Transfer Method (CTLM). Au contacts were defined by lift off lithography. A resin 1813 available commercially was applied by spin coating on the films. Afterwards, the samples were exposed to UV light and the areas for conversion were under covered. All samples were developed with MF311. After this step, gold contacts 400 nm were deposited on the samples by Thermal Evaporation at 10^{-6} Torr. Subsequently, the excess of gold Au was detached from the CTLM structures with acetone. Then, the remaining organic components were removed by washing the samples with Isopropanol and deionized water. Several circles and gaps were measured and averaged during this study with a probe station Cascade Model SUMMIT 11741B-HT. The RBS composition vs depth profile was obtained with 400 keV He+ ions with a beam size about 1 mm. The experimental data was fitted using Analysis IB RBS software 2007 Kobelco. **Figure S6** shows the RBS fitting for each thin film fabricated in this work on sapphire.

ASSOCIATED CONTENT

Supporting Information This material is available free of charge *via* the Internet at http://pubs.acs.org.

AUTHOR INFORMATION

Corresponding author

†*E-mail: mquevedo@utdallas.edu

The authors declare no competing financial interest

ACKNOWLEDGMENTS

The Authors want to thank the National Science Foundation- Division of Electrical, Communications and Cyber Systems (Grant 1139986), Colciencias, Kookmin University, and The Leading Foreign Research Institute Recruitment Program through the National Research Foundation of Korea (NRF) funded by the Ministry of Science, ICT & Future Planning(MSIP) (Grant 2013K1A4A3055679).

AUTHOR CONTRIBUTIONS

The manuscript was written through contributions of all authors. All authors have given approval to the final version of the manuscript

NOTES

The authors declare no competing financial interest.

REFERENCES

1. Bhimanapati, G. R.; Lin, Z.; Meunier, V.; Jung, Y.; Cha, J.; Das, S.; Xiao, D.; Son, Y.; Strano, M. S.; Cooper, V. R.; Liang, L.; Louie, S. G.; Ringe, E.; Zhou, W.; Kim, S. S.; Naik, R.

1
2
3
4
5
6
7
8
9
10
11
12
13
14
15
16
17
18
19
20
21
22
23
24
25
26
27
28
29
30
31
32
33
34
35
36
37
38
39
40
41
42
43
44
45
46
47
48
49
50
51
52
53
54
55
56
57
58
59
60

R.; Sumpter, B. G.; Terrones, H.; Xia, F.; Wang, Y.*et al* . Recent Advances in Two-Dimensional Materials beyond Graphene. *ACS Nano* 2015, 9, 11509-11539.

2. Mak, K. F.; Lee, C.; Hone, J.; Shan, J.; Heinz, T. F. Atomically Thin MoS_2: A New Direct-Gap Semiconductor. *Phys. Rev. Lett.* 2010, 105.

3. Splendiani, A.; Sun, L.; Zhang, Y.; Li, T.; Kim, J.; Chim, C.-Y.; Galli, G.; Wang, F. Emerging Photoluminescence in Monolayer MoS_2. *Nano Lett.* 2010, 10, 1271-1275.

4. Lee, H. S.; Min, S.-W.; Chang, Y.-G.; Park, M. K.; Nam, T.; Kim, H.; Kim, J. H.; Ryu, S.; Im, S. MoS_2 Nanosheet Phototransistors with Thickness-Modulated Optical Energy Gap. *Nano Lett.* 2012, 12, 3695-3700.

5. Chhowalla, M.; Shin, H. S.; Eda, G.; Li, L.-J.; Loh, K. P.; Zhang, H. The Chemistry of Two-dimensional Layered Transition Metal Dichalcogenide Nanosheets. *Nat. Chem.* 2013, 5, 263-275.

6. Tong, X.; Ashalley, E.; Lin, F.; Li, H. D.; Wang, Z. M. M. Advances in MoS_2-Based Field Effect Transistors (FETs). *Nano-Micro Lett.* 2015, 7, 203-218.

7. Li, T. S.; Galli, G. L. Electronic Properties of MoS_2 Nanoparticles. *J. Phys. Chem. C,* 2007, 111, 16192-16196.

8. Yoon, Y.; Ganapathi, K.; Salahuddin, S. How Good Can Monolayer MoS_2 Transistors Be? *Nano Lett.* 2011, 11, 3768-3773.

9. Das, S.; Chen, H. Y.; Penumatcha, A. V.; Appenzeller, J. High Performance Multilayer MoS_2 Transistors with Scandium Contacts. *Nano Lett.* 2013, 13, 100-105.

10. Li, H.; Yin, Z. Y.; He, Q. Y.; Li, H.; Huang, X.; Lu, G.; Fam, D. W. H.; Tok, A. I. Y.; Zhang, Q.; Zhang, H. Fabrication of Single- and Multilayer MoS_2 Film-Based Field-Effect Transistors for Sensing NO at Room Temperature. *Small* 2012, 8, 63-67.

11. Pu, J.; Yomogida, Y.; Liu, K. K.; Li, L. J.; Iwasa, Y.; Takenobu, T. Highly Flexible MoS_2 Thin-Film Transistors with Ion Gel Dielectrics. *Nano Lett.* 2012, 12, 4013-4017.

12. Stephenson, T.; Li, Z.; Olsen, B.; Mitlin, D. Lithium Ion Battery Applications of Molybdenum Disulfide (MoS_2) Nanocomposites. *Energ Environ. Sci.,* 2014, 7, 209-231.

13. Deng, Y. X.; Luo, Z.; Conrad, N. J.; Liu, H.; Gong, Y. J.; Najmaei, S.; Ajayan, P. M.; Lou, J.; Xu, X. F.; Ye, P. D. Black Phosphorus-Monolayer MoS_2 van der Waals Heterojunction p-n Diode. *ACS Nano* 2014, 8, 8292-8299.

14. Wu, W. Z.; Wang, L.; Li, Y. L.; Zhang, F.; Lin, L.; Niu, S. M.; Chenet, D.; Zhang, X.; Hao, Y. F.; Heinz, T. F.; Hone, J.; Wang, Z. L. Piezoelectricity of Single-Atomic-Layer MoS_2 for Energy conversion and piezotronics. *Nature* 2014, 514, 470-474.

15. Radisavljevic, B.; Radenovic, A.; Brivio, J.; Giacometti, V.; Kis, A. Single-Layer MoS_2 Transistors. *Nat Nanotechnol.* 2011, 6, 147-150.

16. Bao, W. Z.; Cai, X. H.; Kim, D.; Sridhara, K.; Fuhrer, M. S. High Mobility Ambipolar MoS_2 field-effect transistors: Substrate and Dielectric Effects. *Appl. Phys. Lett.* 2013, 102.

17. Ganatra, R.; Zhang, Q. Few-Layer MoS_2: A Promising Layered Semiconductor. *ACS Nano* 2014, 8, 4074-4099.

18. Novoselov, K. S.; Jiang, D.; Schedin, F.; Booth, T. J.; Khotkevich, V. V.; Morozov, S. V.; Geim, A. K. Two-Dimensional Atomic Crystals. *P. Natl. Acad. Sci. U.S.A.* 2005, 102, 10451-10453.

19. Castellanos-Gomez, A.; Barkelid, M.; Goossens, A. M.; Calado, V. E.; van der Zant, H. S. J.; Steele, G. A. Laser-Thinning of MoS_2: On Demand Generation of a Single-Layer Semiconductor. *Nano Lett.* 2012, 12, 3187-3192.

20. Wang, X. S.; Feng, H. B.; Wu, Y. M.; Jiao, L. Y. Controlled Synthesis of Highly Crystalline MoS_2 Flakes by Chemical Vapor Deposition. *J. Am. Chem. Soc.* 2013, 135, 5304-5307.

21. Kang, K.; Xie, S. E.; Huang, L. J.; Han, Y. M.; Huang, P. Y.; Mak, K. F.; Kim, C. J.; Muller, D.; Park, J. High-mobility Three-atom-thick Semiconducting Films With Wafer-scale Homogeneity. *Nature* 2015, 520, 656-660.

22. Najmaei, S.; Liu, Z.; Zhou, W.; Zou, X. L.; Shi, G.; Lei, S. D.; Yakobson, B. I.; Idrobo, J. C.; Ajayan, P. M.; Lou, J. Vapour Phase Growth and Grain Goundary Structure of Molybdenum Disulphide Atomic Layers. *Nat. Mater.* 2013, 12, 754-759.

23. Xi, Y.; Serna, M. I.; Cheng, L. X.; Gao, Y.; Baniasadi, M.; Rodriguez-Davila, R.; Kim, J.; Quevedo-Lopez, M. A.; Minary-Jolandan, M. Fabrication of MoS_2 Thin Film Transistors *via* Selective-area Solution Deposition Methods. *J. Mater. Chem. C,* 2015, 3, 3842-3847.

24. Coleman, J. N.; Lotya, M.; O'Neill, A.; Bergin, S. D.; King, P. J.; Khan, U.; Young, K.; Gaucher, A.; De, S.; Smith, R. J.; Shvets, I. V.; Arora, S. K.; Stanton, G.; Kim, H. Y.; Lee, K.; Kim, G. T.; Duesberg, G. S.; Hallam, T.; Boland, J. J.; Wang, J. J. et al. Two-dimensional Nanosheets Produced by Liquid Exfoliation of Layered Materials. *Science* 2011, 331, 568-71.

1
2
3
4
5
6
7
8
9
10
11
12
13
14
15
16
17
18
19
20
21
22
23
24
25
26
27
28
29
30
31
32
33
34
35
36
37
38
39
40
41
42
43
44
45
46
47
48
49
50
51
52
53
54
55
56
57
58
59
60

25. Smith, R. J.; King, P. J.; Lotya, M.; Wirtz, C.; Khan, U.; De, S.; O'Neill, A.; Duesberg, G. S.; Grunlan, J. C.; Moriarty, G.; Chen, J.; Wang, J. Z.; Minett, A. I.; Nicolosi, V.; Coleman, J. N. Large-Scale Exfoliation of Inorganic Layered Compounds in Aqueous Surfactant Solutions. *Adv. Mater.* 2011, 23, 3944-3948.

26. Ambrosi, A.; Sofer, Z.; Pumera, M. Lithium Intercalation Compound Dramatically Influences the Electrochemical Properties of Exfoliated MoS_2. *Small* 2015, 11, 605-612.

27. Lu, J. P.; Lu, J. H.; Liu, H. W.; Liu, B.; Chan, K. X.; Lin, J. D.; Chen, W.; Loh, K. P.; Sow, C. H. Improved Photoelectrical Properties of MoS_2 Films after Laser Micromachining. *ACS Nano* 2014, 8, 6334-6343.

28. Ashfold, M. N. R.; Claeyssens, F.; Fuge, G. M.; Henley, S. J. Pulsed Laser Ablation and Deposition of Thin Films. *Chem. Soc. Rev.* 2004, 33, 23-31.

29. Norton, D. P. Pulsed Laser Deposition of Complex Materials: Progress Toward Applications *In Pulsed Laser Deposition of Thin Films,* John Wiley & Sons, Inc.: 2006; pp 1-31.

30. Zabinski, J. S.; Donley, M. S.; John, P. J.; Dyhouse, V. J.; Safriet, A. J.; Mcdevitt, N. T. Crystallization of Molybdenum-Disulfide Films Deposited by Pulsed Laser Ablation. *Mater. Res. Soc. Symp .P* 1991, 201, 195-200.

31. Donley, M. S.; Murray, P. T.; Barber, S. A.; Haas, T. W. Deposition and Properties of MoS_2 Thin Films Grown by Pulsed Laser Evaporation. *Surf. Coat. Technol.* 1988, 36, 329-340.

32. McDevitt, N. T.; Bultman, J. E.; Zabinski, J. S. Study of Amorphous MoS_2 Films Grown by Pulsed Laser Deposition. *Appl. Spectrosc.* 1998, 52, 1160-1164.

33. Loh, T. A. J.; Chua, D. H. C. Growth Mechanism of Pulsed Laser Fabricated Few-Layer MoS_2 on Metal Substrates. *ACS Appl. Mater. & Interfaces.* 2014, 6, 15966-15971.

34. Serrao, C. R.; Diamond, A. M.; Hsu, S.-L.; You, L.; Gadgil, S.; Clarkson, J.; Carraro, C.; Maboudian, R.; Hu, C.; Salahuddin, S. Highly Crystalline MoS_2 Thin Films Grown by Pulsed Laser Deposition. *Appl. Phys. Lett.* 2015, 106, 052101.

35. Li, X.; Zhu, H. Two-dimensional MoS_2: Properties, preparation, and applications. *J. Materiomics.* 2015, 1, 33-44.

36. Late, D. J.; Shaikh, P. A.; Khare, R.; Kashid, R. V.; Chaudhary, M.; More, M. A.; Ogale, S. B. Pulsed Laser-Deposited MoS_2 Thin Films on W and Si: Field Emission and Photoresponse Studies. *ACS Appl. Mater. & Interfaces.* 2014, 6, 15881-15888.

1
2
3
4
5
6
7
8
9
10
11
12
13
14
15
16
17
18
19
20
21
22
23
24
25
26
27
28
29
30
31
32
33
34
35
36
37
38
39
40
41
42
43
44
45
46
47
48
49
50
51
52
53
54
55
56
57
58
59
60

37. Siegel, G.; Subbaiah, Y. P. V.; Prestgard, M. C.; Tiwari, A. Growth of centimeter-scale atomically thin MoS_2 films by Pulsed Laser Deposition. *APL. Mater.,* 2015, 3.

38. Lee, C.; Yan, H.; Brus, L. E.; Heinz, T. F.; Hone, J.; Ryu, S. Anomalous Lattice Vibrations of Single- and Few-Layer MoS_2. *ACS Nano.* 2010, 4, 2695-2700.

40. Buscema, M.; Steele, G.; van der Zant, H. J.; Castellanos-Gomez, A. The effect of the substrate on the Raman and Photoluminescence Emission of Single-layer MoS_2. *Nano Res.* 2014, 7, 561-571.

41. Boyd, I. W. Thin film Growth by Pulsed Laser Deposition. *Ceram Int* 1996, 22, 429-434.

42. Greer, J. Large-Area Commercial Pulsed Laser Deposition. In *Pulsed Laser Deposition of Thin Films*, John Wiley & Sons, Inc.: 2006; pp 191-213.

43. Jabri, S.; Souissi, H.; Souissi, A.; Meftah, A.; Sallet, V.; Lusson, A.; Galtier, P.; Oueslati, M. Investigation of the Vibrational Modes of ZnO grown by MOCVD on Different Orientation Planes. *J.Raman Spectros.* 2015, 46, 251-255.

44. Donarelli, M.; Bisti, F.; Perrozzi, F.; Ottaviano, L. Tunable Sulfur desorption in Exfoliated MoS_2 by Means of Thermal Annealing in Ultra-high Vacuum. *Chem. Phys. Lett.* 2013, 588, 198-202.

45. Kim, S.; Konar, A.; Hwang, W.-S.; Lee, J. H.; Lee, J.; Yang, J.; Jung, C.; Kim, H.; Yoo, J.-B.; Choi, J.-Y.; Jin, Y. W.; Lee, S. Y.; Jena, D.; Choi, W.; Kim, K. High-mobility and low-Power Thin-Film Transistors Based on Multilayer MoS_2 Crystals. *Nat Commun.* 2012, 3, 1011.

46. Wang, Q. H.; Kalantar-Zadeh, K.; Kis, A.; Coleman, J. N.; Strano, M. S. Electronics and Optoelectronics of Two-dimensional Transition Metal Dichalcogenides. *Nat Nano.* 2012, 7, 699-712.

47. Kang, K.; Xie, S.; Huang, L.; Han, Y.; Huang, P. Y.; Mak, K. F.; Kim, C.-J.; Muller, D.; Park, J. High-mobility Three-atom-thick Semiconducting Films with Wafer-scale Homogeneity. *Nature* 2015, 520, 656-660.

48. Choi, K.; Raza, S. R. A.; Lee, H. S.; Jeon, P. J.; Pezeshki, A.; Min, S.-W.; Kim, J. S.; Yoon, W.; Ju, S.-Y.; Lee, K.; Im, S. Trap Density Probing on Top-gate MoS_2 Nanosheet Field-Effect Transistors by Photo-excited Charge Collection Spectroscopy. *Nanoscale* 2015, 7, 5617-5623.

49. Magda, G. Z.; Pető, J.; Dobrik, G.; Hwang, C.; Biró, L. P.; Tapasztó, L. Exfoliation of Large-area Transition Metal Chalcogenide Single Layers. *Sci Rep.* 2015, 5, 14714.

50. Zhan, Y.; Liu, Z.; Najmaei, S.; Ajayan, P. M.; Lou, J. Large-Area Vapor-Phase Growth and Characterization of MoS_2 Atomic Layers on a SiO_2 Substrate. *Small* 2012, 8, 966-971.

51. Liu, D.; Guo, Y.; Fang, L.; Robertson, J. Sulfur Vacancies in Monolayer MoS_2 and its Electrical Contacts. *Appl. Phys. Lett.* 2013, 103, 183113.

52. Van der Zande, A. M.; Huang, P. Y.; Chenet, D. A.; Berkelbach, T. C.; You, Y.; Lee, G.-H.; Heinz, T. F.; Reichman, D. R.; Muller, D. A.; Hone, J. C. Grains and Grain Boundaries in Highly Crystalline Monolayer Molybdenum Disulphide. *Nat Mater.* 2013, 12, 554-561.

TABLE OF CONTENTS GRAPHIC AND SYNOPSIS